

## Quantitative prediction of injected CO<sub>2</sub> at Sleipner using wave-equation based AVO

Haffinger, Peter; Jedari Eyvazi, Farid; Doulgeris, P.; Steeghs, P.; Gisolf, Dries; Verschuur, Eric

**Publication date**

2017

**Document Version**

Final published version

**Published in**

First Break

**Citation (APA)**

Haffinger, P., Jedari Eyvazi, F., Doulgeris, P., Steeghs, P., Gisolf, D., & Verschuur, E. (2017). Quantitative prediction of injected CO<sub>2</sub> at Sleipner using wave-equation based AVO. *First Break*, 35, 65-70.

**Important note**

To cite this publication, please use the final published version (if applicable).  
Please check the document version above.

**Copyright**

Other than for strictly personal use, it is not permitted to download, forward or distribute the text or part of it, without the consent of the author(s) and/or copyright holder(s), unless the work is under an open content license such as Creative Commons.

**Takedown policy**

Please contact us and provide details if you believe this document breaches copyrights.  
We will remove access to the work immediately and investigate your claim.

# Quantitative prediction of injected CO<sub>2</sub> at Sleipner using wave-equation based AVO

Peter Haffinger<sup>1\*</sup>, Farid Jedari Eyvazi<sup>2</sup>, Panos Doulgeris<sup>1</sup>, Philippe Steeghs<sup>3</sup>, Dries Gisolf<sup>1</sup> and Eric Verschuur<sup>4</sup> demonstrate a wave-equation technique on a seismic dataset at the Sleipner site.

## Introduction

In the context of carbon capture and storage (CCS), quantitative estimation of injected CO<sub>2</sub> is of vital importance to verify if the process occurs without any leakage. From a geophysical perspective this is challenging as a CO<sub>2</sub> plume has a severe imprint on seismic data. While this makes delineation of the plume rather straightforward, for quantitative interpretation a technique is required that takes complex wave propagation, including multiple scattering and mode conversions into account. In this contribution to the Special Topic, a wave-equation based AVO technique is discussed and successfully demonstrated on a seismic dataset from the Sleipner site. The technique solves the exact wave-equation which means that all complex wave propagation effects mentioned above are properly modelled. The scheme naturally inverts for compressibility and shear compliance and these parameters are more closely related to saturation, porosity and lithology than the conventional impedances. From compressibility the CO<sub>2</sub> saturation can be found and the total amount of injected CO<sub>2</sub> is calculated by integration over the plume. The result obtained was found to be in good agreement with the known value at the time when the data was acquired.

Permanent storage of CO<sub>2</sub> in the subsurface may provide an important contribution to climate change mitigation. In 1996 the first CO<sub>2</sub> was injected into the Utsira Formation above the Sleipner gas field in the North Sea. Now, about 20 years later, injection is still being done at Sleipner, which makes the Sleipner project not only the first, but also the longest-running industrial-scale aquifer CO<sub>2</sub> storage project. In the period 1996-2014 a total of eight repeated 3D time-lapse seismic surveys have been acquired. These data have not only provided important feedback on the storage reservoir behaviour, but have also been vital for the development of CO<sub>2</sub> monitoring in general.

As of today more than 150 papers have been published about the Sleipner CO<sub>2</sub> monitoring scheme. The majority of these focus on the time-lapse seismic interpretation and reservoir characterization with increasingly sophisticated approaches (Furre et al., 2015; Raknes et al., 2015). One of the geophysical challenges for CO<sub>2</sub> monitoring is that the injected gas creates very high amplitudes on seismic data with a notable superposition of reflections from different layers. The complex wave-propagation cannot really be explained by conventional linear AVO or imaging methods and a wave-equation-based

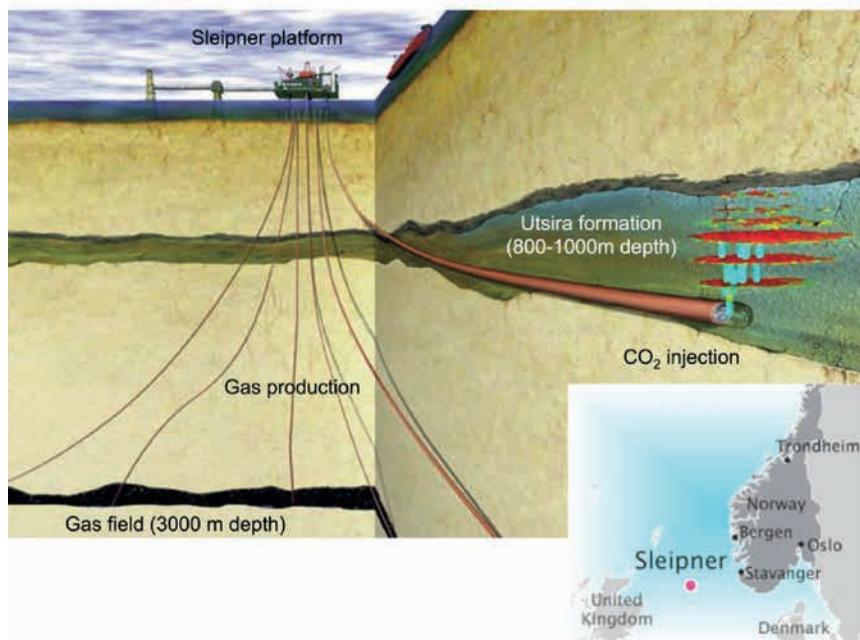


**Figure 1** Location of the Sleipner gas field and the geological set-up. Natural gas is produced from a 3000m-deep reservoir while re-injection of the produced CO<sub>2</sub> occurs in the much shallower Utsira formation.

<sup>1</sup> Delft Inversion, Delft, The Netherlands | <sup>2</sup> GESciTech, London, United Kingdom | <sup>3</sup> TNO, Utrecht, The Netherlands |

<sup>4</sup> University of Technology, Delft, The Netherlands

\* Corresponding author, E-mail: haffinger@delft-inversion.com

approach should be used to account for all these effects in the seismic in order to obtain absolute estimates of the stored CO<sub>2</sub>.

**Study area and geological setup**

The Sleipner field is located in the North Sea with an approximate distance of 260 km to the Norwegian coastline. The field is operated by Statoil, with natural gas production starting in the late 1970s. The gas is produced from reservoir formations at 2500-3000 m depth. At surface conditions it turns out that as a side product also up to 9% carbon dioxide is produced, which has to be reduced to a maximum of 2.5% in order to meet export specifications and customer requirements. After separating the necessary amount, the CO<sub>2</sub> is re-injected into the subsurface, the Utsira formation, which is located at a much shallower depth (800-1000 m) compared to the original reservoir.

While the total amount of injected CO<sub>2</sub> is known as a function of time, from a safety and regulatory perspective it is highly desirable to know if the entire CO<sub>2</sub> remains stored in the target formation without any leakage through the cap rock. This geophysical challenge can be addressed by seismic methods, but to comply truly with the requirements, the derived information has to be quantitative. Unfortunately, this is an intrinsic limitation of conventional seismic AVO techniques. Standard AVO methods are routinely based on the linearised Zoeppritz equations and as a consequence they result in band-limited reservoir properties only. In addition, they are unable to handle the complex wave propagation inside the CO<sub>2</sub> plume. In order to estimate quantitatively the CO<sub>2</sub> in place we utilize a wave-equation based AVO technique in this study (WEB-AVO), which has the potential to recover spatially broadband reservoir properties from temporally band-limited seismic data.

**WEB-AVO: A wave-equation-based AVO technology**

In this chapter we demonstrate a wave-equation based AVO (WEB-AVO) technology (e.g., Gisolf and van den Berg, 2012) for quantitative interpretation of the CO<sub>2</sub> plume injected into the Sleipner field. The full elastic wave-equation is solved iteratively and as a consequence, multiple scattering and mode conversions over the target interval are properly accounted for. In addition, the inherent de-tuning of the seismic amplitudes in the inversion gives a reservoir model with a spatial bandwidth wider than what could be expected from the temporal bandwidth of the seismic data. Starting with an incident field in a smooth background model, a first estimate of the reservoir model is obtained, under the assumption of a linear relationship between elastic subsurface properties and seismic amplitudes. In the next step, the wave-equation is deployed to include second-order scattering based on the first estimate of the reservoir properties. The full scheme consists of an iterative procedure of AVO inversions, using the best estimate of the wave-field in the reservoir, followed by updating the wave-field based on the latest reservoir model. The procedure is repeated until neither the reservoir model nor the wave-field changes any more and

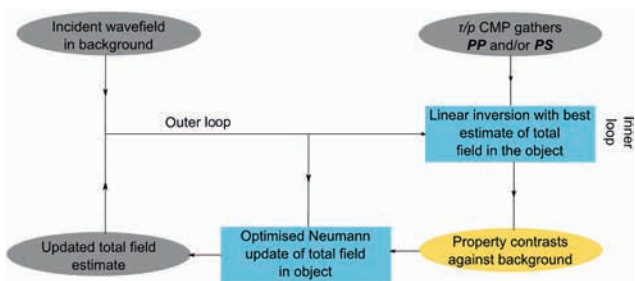


**Figure 2** Block diagram to visualize WEB-AVO and the involved processes schematically.

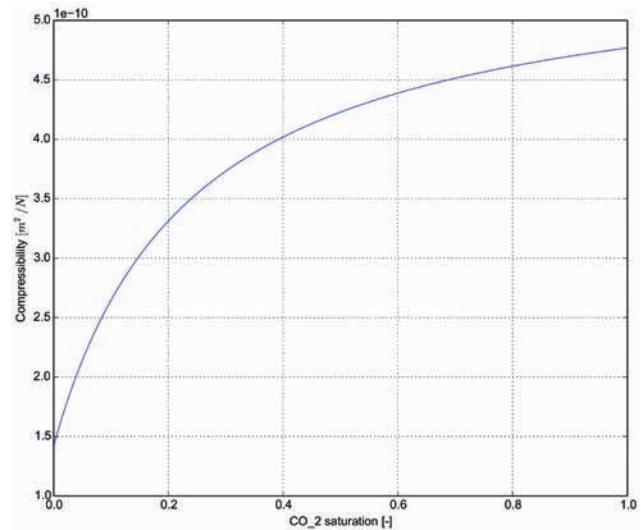


**Figure 3** Relationship between compressibility and saturation for a porosity of 0.36 and a CO<sub>2</sub> density of 600 kg/m<sup>3</sup>. The relationship was derived from the Gassmann equations and will be used to translate the inverted compressibilities into CO<sub>2</sub> saturation.

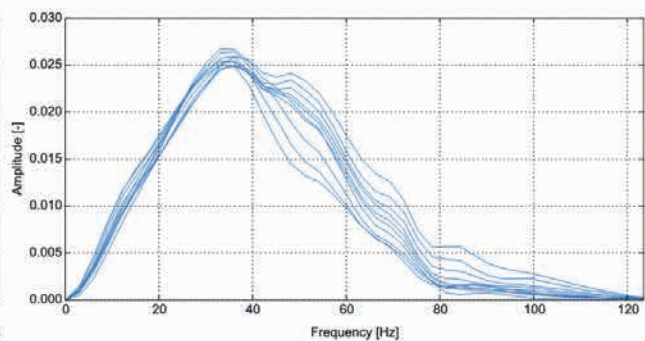
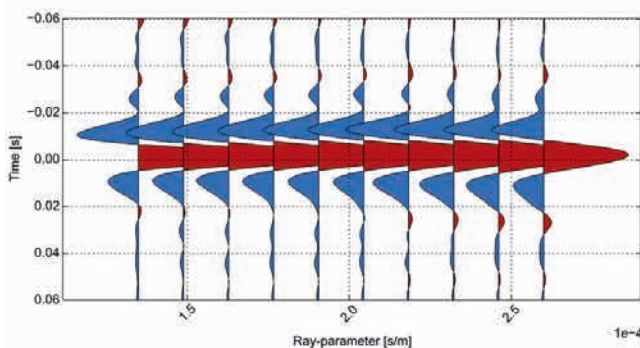


**Figure 4** Slowness-dependent wavelets were estimated by tying the seismic to well 15/9-13. The wavelets show a slightly negative phase rotation and the center frequency appears at f = 35 Hz.

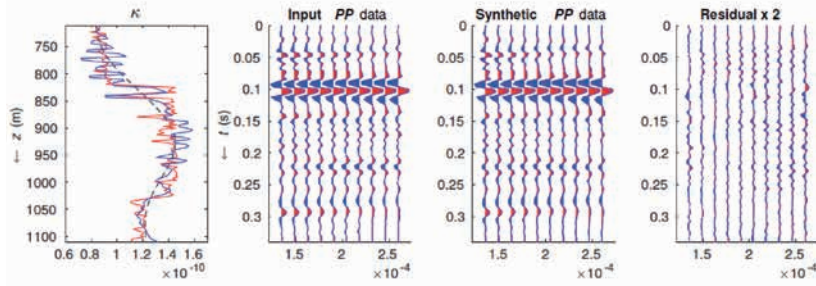
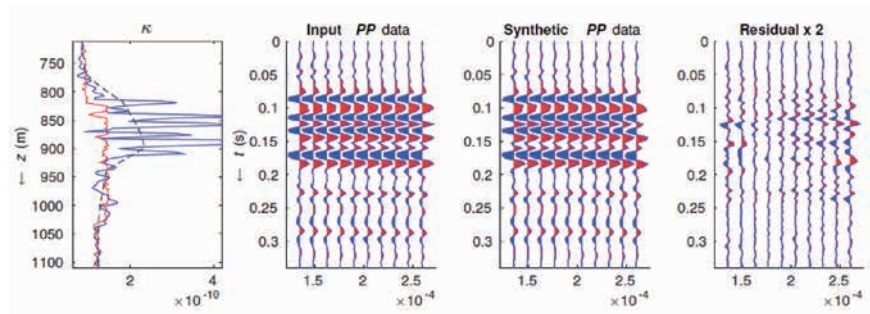


**Figure 5** The inverted compressibility (blue), the logged compressibility (red) from well 15/9-13 and the background model (black). The predicted synthetic data matches the input seismic very well. The main event in time is translated into the correct thickness in depth demonstrating the intrinsic de-tuning of WEB-AVO. It should be realized that well 15/9-13 is located outside the plume while inside the compressibilities will be significantly higher than the values shown.

**Figure 6** Same panels as in Figure 5 but now for a CMP location inside the plume. The red curve is the compressibility from well 15/9-13 and only serves as a reference here. The inversion result in blue confirms that after CO<sub>2</sub> injection the compressibility is significantly increased. Six individual sand layers with CO<sub>2</sub> in the pores can be identified. As previously, the data has been predicted very well by the technology. This is confirmed by the low residual shown in the right panel.



convergence is reached. A schematic depiction of the procedure is shown in Figure 2.

Another unique feature of the method is that it solves directly for compressibility (inverse of bulk modulus) and shear compliance (inverse of shear modulus) instead of impedances as obtained by conventional linear AVO techniques. Gisolf (2016) demonstrated that compressibility and shear compliance are highly suitable for quantitative interpretation as they are much more sensitive to porosity and fluid changes compared to acoustic and shear impedance.

### Target-oriented AVO

While adding value at several stages of seismic interpretation, the computational costs of solving the wave equation grow strongly with the number of grid cells of the inversion domain. To keep the process feasible, the scheme is applied in a target-oriented mode covering a depth interval of approx. 500 m. The exact depth interval is dependent on the vertical depth sampling, which in turn depends on the maximum frequency in the seismic data and the lowest velocity over the target.

Being target-oriented implies that only multiple scattering and mode conversions that are generated over the target interval are properly predicted by the methodology. At the same time, overburden- and surface-related multiples should be removed from the input data by standard processing or, preferably, by full wave-field processing. While linear AVO techniques inevitably misinterpret these types of events, WEB-AVO has a tendency to reject this noise as it does not obey the target-oriented wave-equation. This makes the technology very robust even in set-ups with low S/N or where older seismic data is available only, which initially was not shot for the primary purpose of quantitative interpretation studies.

### Data input and preparation

In this study, we used well 15/9-13 to derive seismic wavelets, which are needed as input to the inversion. This step also calibrates the seismic data with respect to angle-dependent

propagation effects in the overburden. While only sonic and gamma-ray were genuinely logged, shear sonic and density were derived following the method proposed by Delépine et al. (2011). From this set of logs, compressibility  $\kappa$  and shear compliance  $M$  were computed. The seismic wavelets obtained, together with their frequency spectra, are displayed in Figure 4. Seismic input were three offset stacks from 3D time-migration, which were interpolated to ten regular slownesses, since the wave-equation, and consequently also our inversion approach, is formulated in this domain. The chosen slownesses translate to an angle range of approx. 16-31 degrees at target depth. This step requires the migration velocity model and assumes horizontal stratification of the overburden. To remove dipping noise from the migrated sections (acquisition imprint, migration artefacts, etc.), a mild-dip filter was applied, resulting in a slightly improved S/N of the input seismic. As a starting point the inversion needs background models for  $\kappa$ ,  $M$  and  $\rho$ . Outside the plume these backgrounds were equal to a very smooth version ( $f_{\max} = 4$  Hz) of the 15/9-13 logs, while inside the plume the background values were scaled versions consistent with Gassmann modelling. This procedure requires a rough delineation of the plume based on the energy in the seismic data, but since the CO<sub>2</sub> strongly affects the amplitudes this is a straightforward exercise. In Figure 3 the relationship between CO<sub>2</sub> saturation and compressibility is shown assuming a porosity  $\phi$  of 0.36 (Singh et al., 2010) and a CO<sub>2</sub> density  $\rho_{\text{CO}_2}$  of 600 kg/m<sup>3</sup>.

### Results

WEB-AVO was applied to a 3D volume of the 2008 survey with a total surface coverage of approx. 11 km<sup>2</sup>. The target interval with a length of 400 m included the Utsira formation and was sampled on a 3 m grid for the inversion. Although a simultaneous two-parameter ( $\kappa$ ,  $M$ ) inversion was performed, here we focus on the compressibility as it is the relevant parameter for quantitative prediction of CO<sub>2</sub> saturation, while the shear compliance  $M$  is independent of the pore fill. This is an intrinsic benefit of formulating the inversion in terms of compressibility and shear



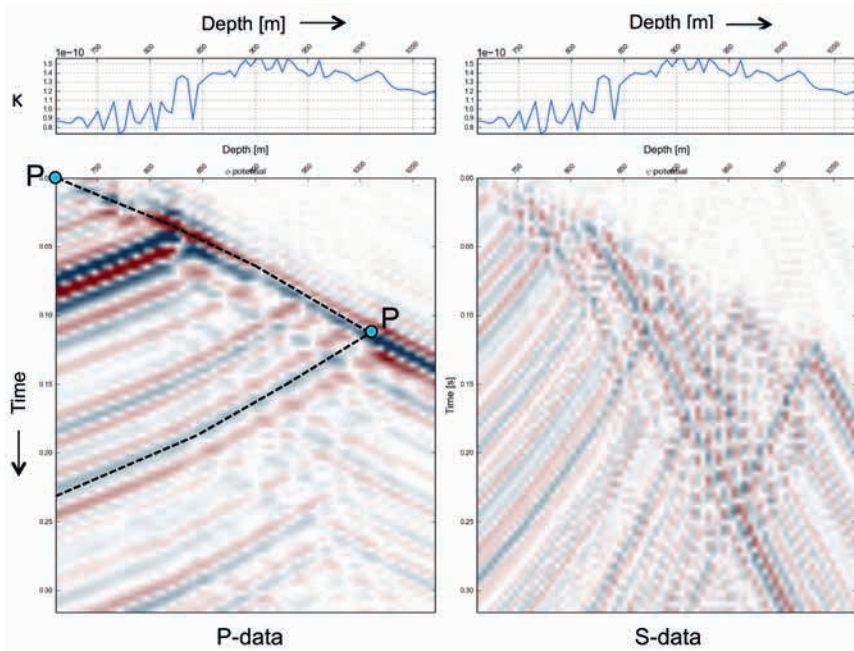


**Figure 7** Total wave-field estimated by WEB-AVO at the well location 15/9-13. The field is decomposed into its P-component (left panel) and S-component (right panel). Similar to the way VSP-data is displayed the vertical axis is time and the horizontal axis is depth. The ray-path for an exemplary PP-primary is drawn into the left panel.

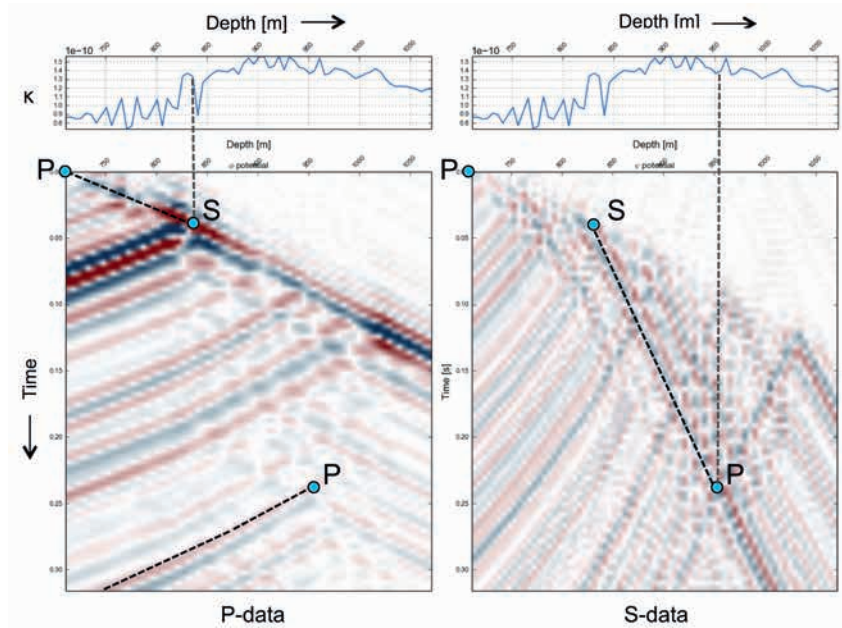


**Figure 8** Same display as Figure 7 but now with the interpretation of a PSP-converted wave.

compliance. In Figure 5 the inversion result for  $\kappa$  is shown at well location 15/9-13.

It can be said that the inverted compressibility (blue curve) matches well with the ‘logged’ compressibility (red curve). The top and base of the Utsira formation are nicely recovered by WEB-AVO and an internal structure of alternating sand and shale layers can be interpreted. The strong shale break at  $z = 850$  m is particularly prominent. One should keep in mind that the logs for well 15/9-13 were mainly derived from gamma-ray measurements and correlations with other well data that was available in the area. While for wavelet extraction the logs proved to be sufficient, they should not be considered as the ground truth. Taking this into account the match between the two curves can probably be appreciated even more.

In the next step WEB-AVO was applied to a CMP location inside the plume. The results are displayed in Figure 6. Looking at

the seismic input data alone (second panel from the left) it becomes very clear already that much more is going on here. While outside the plume the seismic signal is dominated by a single event, the top of the Utsira formation, inside the plume several strong amplitudes can be found. These strong seismic events are a result of extremely high contrasts/reflectivities, which characterize the subsurface after injection of  $\text{CO}_2$ . The inverted compressibility confirms this statement as the recovered properties (blue curve) inside the plume clearly exceed the logged values outside the plume and measured in well 15/9-13 (red curve).

Before we apply WEB-AVO to the full 3D seismic volume we will investigate the role of complex wave-propagation, hence multiple scattering and mode conversions in the process. Another benefit of solving the wave-equation is that the computed total wave-field at any point inside the inversion domain can be displayed and interpreted. Since we are dealing with a 1.5D inversion

scheme here, an appropriate way to visualize the total wave-field is to use a VSP-type display. The wave-field as estimated at the well location outside the plume is shown in Figure 7. In order to be able to see the scattered events better, the incident wave-field propagating in the background has been subtracted from the total wave-field. The resulting field is called the scattered field.

It should be realized that, similar to the way VSP data is commonly displayed, the vertical axis represents time while the horizontal axis denotes depth. Furthermore, the total wave-field is decomposed into its P-component, shown in the left panel, and its S-component, shown in the right panel. Interpretation of Figure 7 allows for better understanding of potential multiple scattering and mode conversions. All events dipping to the right are downward propagating waves while all data dipping to the left are upward propagating waves. The strong and downward-dipping event on the P-panel is the primary forward scattered energy following the path of the incident wave that is generated by the seismic source. The ray-path of a simple PP-primary is drawn with a dashed line and the reflection point is indicated by the blue dot inside the panel.

Figure 8 is in principle a duplicate of Figure 7 but now with the interpretation of a PSP-converted wave. It all starts again with the downward propagating incident P-wavefield. While a strong P-reflection is generated at the top of the Utsira formation, a converted wave also is generated. This PS-conversion can now be followed on the right panel where the S-components are shown. The converted S-wave is dipping to the right, which implies that it is still propagating downward. The conversion from P to S consequently occurred as a result of transmission. Following this type of interpretation, we can also understand the P to S conversion in reflection, which occurs deeper in the section. Note that the created upward propagating P-event arrives at a travelttime that falls outside the window that was used for inversion. Still, it is interesting to be able to demonstrate that these complex wave phenomena are truly predicted by the inversion engine and should therefore lead to improved reservoir characterization results. The authors do realize that conventional seismic data processing

does aim at removing dipping and curved events from pre-stack gathers. Converted waves that are generated over the inversion interval could well fall into this category.

Therefore, the consequences of seismic data pre-conditioning should be well understood as they could potentially lead to different pre-processing schemes when wave-equation-based AVO inversion is aimed for. To conclude the current investigation, we show the scattered wave-field for the location inside the plume in Figure 9. The reader should be able by now to perform his own interpretation of the different wave modes. It is interesting to realize that inside the CO<sub>2</sub> plume wave-propagation appears to be much more dominated by internal multiple scattering (intrinsic P-multiples) compared to mode conversions. Internal scattering is very prominent inside the depth interval that is defined by CO<sub>2</sub> accumulation, as can be expected. In the bottom-right corner of the P-data panel, a notable amount of downward propagating energy can be identified, which is an easy QC for the role internal P-multiples play in a given set-up. If no internal scattering occurred, the bottom right corner should not show any energy since the incident wave-field would be the only downward propagating wave. This concludes discussion of inversion results for individual CMP locations and we will now continue with the inversion results of the 3D seismic volume.

From the  $\kappa$  predictions obtained over the whole volume, a geobody can be extracted to delineate the extent of the CO<sub>2</sub> at the time when the seismic data was acquired (2008). Figure 10 shows the background model and the inversion result for  $\kappa$  along a cross-line and an in-line as well as the extracted 3D geobody. Within the geobody, CO<sub>2</sub> saturation can then be predicted using the relationship given in Figure 3. The total mass of CO<sub>2</sub> in place follows naturally from the inversion grid ( $\Delta x; \Delta y; \Delta z$ ) and the porosity  $\phi = 0.36$  as:

$$\begin{aligned}
 m_{CO_2} &= \sum_{grid} \phi \rho_{CO_2} \sigma_{CO_2} \Delta x \Delta y \Delta z \\
 &= \sum_{grid} 0.36 \cdot 600 \frac{kg}{m^3} \cdot \sigma_{CO_2} \cdot 25m \cdot 25m \cdot 3m \\
 &= 12.1 Mt
 \end{aligned}$$

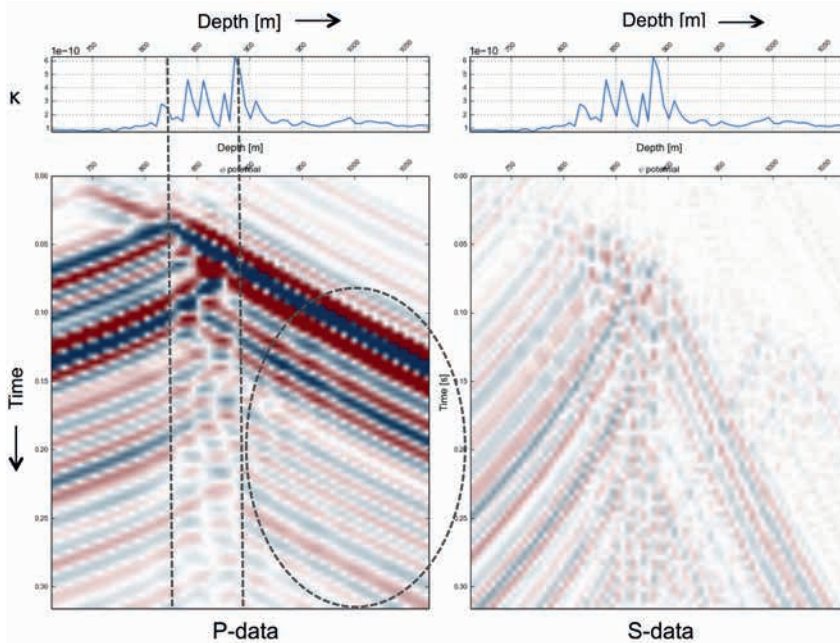


**Figure 9** Same display as Figure 7 but now for a location inside the plume. The area indicated by the oval shows strong internal multiples.

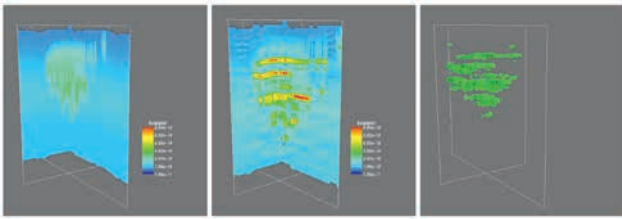


**Figure 10** Shown is the background model for compressibility (left) as well as the inversion result for the same parameter (middle). By defining a cut-off value, a 3D geobody can be extracted in order to delineate the CO<sub>2</sub> plume. In this case a cut-off value for  $\kappa$  of  $2.72 \times 10^{-10}$  m<sup>2</sup>/N was used.

where the density of CO<sub>2</sub> at reservoir conditions  $\rho_{\text{CO}_2}$  was assumed to be 600 kg/m<sup>3</sup>, which is an average of the expected values. It is known that this parameter can vary notably owing to the CO<sub>2</sub> being close to its critical point [Alnes et al. (2011)] and having a clear understanding of the density distribution within the plume would be an advantage. With around 11 Mt of CO<sub>2</sub> injected by 2008, this is a very good estimate, although the total amount is slightly overestimated. In Figure 10 it can be seen that the inverted compressibility, at least locally, exceeds  $4.75 \times 10^{-10}$  m<sup>2</sup>/N, which was predicted for 100% CO<sub>2</sub> saturation. This can possibly be explained by variations in the porosity or the CO<sub>2</sub> density. Estimation of these parameters in 3D would be worthwhile in order to specify the amount more precisely.

### Summary and discussion

In this publication a wave-equation-based AVO technique (WEB-AVO) was discussed and successfully demonstrated on a 3D seismic dataset from the Sleipner field. The method inverts migrated seismic data in time for absolute reservoir properties (compressibility and shear compliance) in depth. Since the wave-equation is solved, tuning effects owing to internal scattering and mode conversion are correctly handled by the process. Using rock-physics modelling, the obtained compressibilities were translated into a saturation model. A total amount of 12.1 Mt CO<sub>2</sub> was calculated as being stored in the area, which is in good agreement with the expected value of 11 Mt.

For carbon capture and storage, and for underground storage in general, the amount of injected CO<sub>2</sub> (gas) is known beforehand. The geophysical challenge then becomes to investigate if the entire amount is stored safely and securely and without any leakage. While the proposed workflow was successfully applied in this context, several other cases can be thought of, to which WEB-AVO could add value:

- Reserves estimation for improved field development planning.
- Time-lapse monitoring (4D) to accurately understand changes in fluid properties over time.
- Optimize well planning by using compressibility as a direct hydrocarbon indicator (e.g. Beller et al., 2015).

Application of wave-equation-based AVO in time-lapse mode is very relevant for Sleipner, where several surveys from different acquisition years are available. The technology discussed is highly suitable for 4D monitoring, because the compressibility is most sensitive to changes in pore fill, while the shear compliance only reacts to changes in lithology. Assuming that the lithology will not change for different seismic acquisitions, a simultaneous 4D inversion would be needed for one shear compliance only, independent of the number of surveys. This reduces the number of unknown reservoir parameters, representing a clear advantage of the demonstrated technology compared to conventional AVO methods, which are usually formulated in terms of impedances. Application of wave-equation-based AVO for simultaneous inversion of time-lapse data will be part of future field applications.

### Acknowledgements

We would like to thank the licenceholders of PL046 (Statoil, Lotos, ExxonMobil, Total) for making the data available and for their permission to publish this work.

### References

- Alnes, H., Eiken, O., Nooner, S., Sasagawa, G., Stenvold, T. and Zumberge, M. [2011]. Results from Sleipner gravity monitoring: Updated density and temperature distribution of the CO<sub>2</sub> plume. *10th International Conference on Greenhouse Gas Control Technologies*, Volume 4, 5504-5511.
- Beller, M., Dougeris, P., Gisolf, A., Haffinger, P., Huis in't Veld, R. and Wever, A.K.T. [2015]. Resolving Carboniferous Stacked Channel Sequences with a Non-linear AVO Technology. *77th EAGE Conference and Exhibition*, Extended Abstracts.
- Delépine, N., Clochard, V., Labat, K. and Ricarte, P., [2011]. Post-stack stratigraphic inversion workflow applied to carbon dioxide storage: Application to the saline aquifer of Sleipner field. *Geophysical Prospecting*, **59** (1), 132-144.
- Furre, A.K., Kiær, A. and Eiken, O., [2015]. CO<sub>2</sub>-induced seismic time shifts at Sleipner. *Interpretation*, **3** (3), SS23-SS35.
- Gisolf, A. [2016]. Parameterisation for Reservoir Oriented AVO Inversion, *78th EAGE Conference and Exhibition*, Extended Abstracts.
- Gisolf, A. and van den Berg, P.M. [2012]. Target-oriented Elastic Full Wave Form Inversion. *74th EAGE Conference and Exhibition*, Extended Abstracts.
- Raknes, E.B., Arntsen, B., and Weibull, W., [2015]. Three-dimensional elastic full waveform inversion using seismic data from the Sleipner area. *Geophys. J. Int.*, **202**, 1877-1894.
- Singh, V., Cavanagh, A., Hansen, H., Nazarian, B. Iding, M. and Ringrose, P. [2010]. Reservoir Modeling of CO<sub>2</sub> Plume Behavior Calibrated Against Monitoring Data From Sleipner, Norway. *SPE Annual Technical Conference and Exhibition*, Expanded Abstracts.